Cysteine-to-Serine Mutants of the Human Copper Chaperone for Superoxide Dismutase Reveal a Copper Cluster at a Domain III Dimer Interface†

Jay P. Stasser,‡ John F. Eisses,§ Amanda N. Barry,‡ Jack H. Kaplan,§ and Ninian J. Blackburn*,‡

Department of Environmental and Biomolecular Systems, OGI School of Science & Engineering, Oregon Health & Science University, Beaverton, Oregon 97006, and Department of Biochemistry & Molecular Genetics, University of Illinois at Chicago, Chicago, Illinois 60607

Received October 7, 2004; Revised Manuscript Received November 25, 2004

ABSTRACT: Cysteine-to-serine mutants of a maltose binding protein fusion with the human copper chaperone for superoxide dismutase (hCCS) were studied with respect to (i) their ability to transfer Cu to E,Zn superoxide dismutase (SOD) and (ii) their Zn and Cu binding and X-ray absorption spectroscopic (XAS) properties. Previous work has established that Cu(I) binds to four cysteine residues, two of which, C22 and C25, reside within an Atox1-like N-terminal domain (DI) and two of which, C244 and C246, reside in a short unstructured polypeptide chain at the C-terminus (DIII). The wild-type (WT) protein shows an extended X-ray absorption fine structure (EXAFS) spectrum characteristic of cluster formation, but it is not known how such a cluster is formed. Cys to Ser mutagenesis was used to investigate the Cu binding in more detail. Single Cys to Ser mutations, as represented by C22S and C244S, did little to affect the metal binding ratios of hCCS. Both mutants still showed approximately 2 Cu(I) ions and 1 Zn ion per protein. The double mutants C22/24S and C244/246S, on the other hand, showed Cu binding stoichiometries close to 1:1. The Zn-EXAFS of WT CCS showed a 3−4 histidine ligand environment that is consistent with Zn binding in the SOD-like domain II of CCS. The Zn environment remained unchanged between wild type and all of the mutant CCS proteins. Single Cys to Ser mutations displayed lower activity than WT protein, although close to full activity could be rescued by increasing the CCS:SOD ratios to 8:1 in the assay mixture. The structure of the Cu centers of the single mutants as revealed by EXAFS was also similar to that of WT protein, with clear indications of a Cu cluster. On the other hand, the double mutants showed a greater degree of perturbation. The DI C22/25S mutant was 70% active and formed a cluster with a more intense Cu−Cu interaction. The DIII C244/246S mutant retained only a fraction (16%) of activity and did not form a cluster. The results suggest the formation of a DIII−DIII cluster within a dimeric or tetrameric protein and further suggest that this cluster may be an important element of the copper transfer machinery.

Copper chaperones are a class of proteins that sequester and deliver copper to specific target enzymes that utilize copper in their active sites. In the cell, free Cu(I) is oxidized to Cu(II) and can undergo Fenton-like reactions, which can generate radicals that may react with and oxidize larger biopolymers and membrane lipids (*1*). Whereas cells must maintain sufficient levels of total cytosolic copper, free uncomplexed copper is very low, estimated to be less than one copper atom per cell (*2*, *3*). Copper chaperones provide a dual function, ensuring adequate copper supply to their target proteins from the pool of complexed cytosolic copper and also protecting the cell from the possible toxic effects of free copper ions. Many copper chaperones have been discovered in the human cell, including the chaperone for Wilson and Menkes disease proteins, Atox1 (*4*−*9*), the copper chaperones for cytochrome *c* oxidase, SCO1 (*10*−*12*), COX11 (*13*−*15*), and COX17 (*16*−*19*), and the copper chaperone for superoxide dismutase, CCS[1] (*20*−*24*).

Cu,Zn superoxide dismutase (SOD) is the target enzyme of CCS. SOD is a 32 kDa homodimeric protein that contains a redox-active Cu site and a structural Zn site (*25*, *26*). SOD catalyzes the disproportionation of the superoxide anion (*27*), a toxic byproduct of oxygen chemistry. The Cu(II) ion in SOD is bound to four histidines and one solvent molecule, while the zinc ion is bound to three histidines and one aspartate residue. On reduction the Cu(I) center becomes

† The work was supported by a program project grant from the National Institutes of Health (P01 GM067166) to N.J.B. and J.H.K. Stanford Synchrotron Radiation Laboratory is supported by the National Institutes of Health Biomedical Research Technology Program, Division of Research Resources, and by the U.S. Department of Energy, Basic Energy Sciences (BES), and Office of Biological and Environmental Research.

* To whom correspondence should be addressed at the Department of Environmental and Biomolecular Systems, OGI School of Science & Engineering at OHSU, 20000 NW Walker Rd., Beaverton, OR 97006-8921. Phone (503) 748-1384; fax (503) 748-1464; e-mail ninian@ebs.ogi.edu.

‡ Oregon Health & Science University.

§ University of Illinois at Chicago.

[1] Abbreviations: CCS, copper chaperone for superoxide dismutase; DI, DII, and DIII, domains I, II, and III; DW, Debye−Waller factor; EXAFS, extended X-ray absorption fine structure; FT, Fourier transform; hCCS, human copper chaperone for superoxide dismutase; SOD, superoxide dismutase; WT, wild type; XAS, X-ray absorption spectroscopy; XANES, X-ray absorption near edge structure; yCCS, yeast copper chaperone for superoxide dismutase.

10.1021/bi0478392 CCC: $30.25
Published on Web 02/11/2005

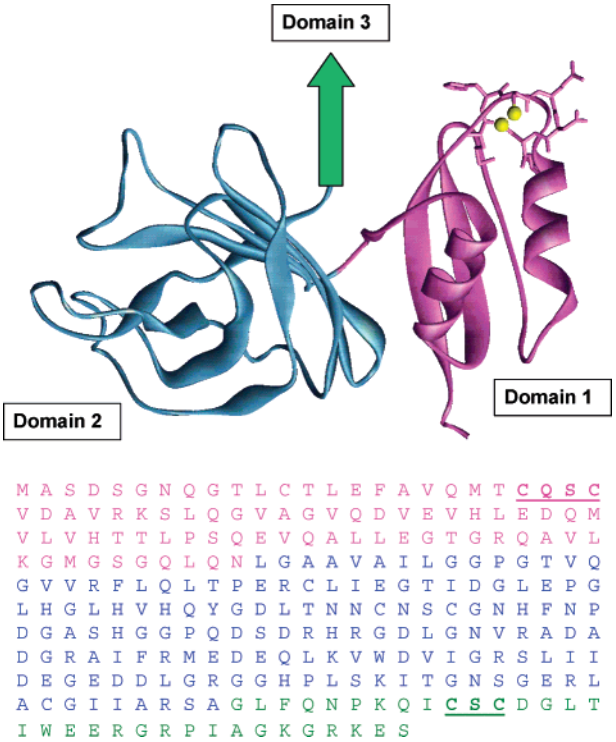

FIGURE 1: Domain structure of CCS. The figure shows a ribbon diagram of the crystal structure of yCCS (PDB file 1QUP) with domain I (DI) shown in magenta and domain II (DII) shown in blue. Domain III (DIII), which is disordered in the crystal structure, is represented by the green arrow. The sequence of human CCS corresponding to the three domains is shown below with the same color code. The metal-binding cysteine motifs are underlined.

3-coordinate, losing a water and the bridging imidazolate ligand (*28*). One of the unusual features of Cu,Zn SOD is its strong dimer interface. The dimerization of SOD has been shown to resist temperatures of up to 100 °C, 8 M urea, and 1% SDS (*29*).

Unlike its target, CCS is a three-domain protein (Figure 1) (*21*−*23*, *30*). Domain I (DI, residues 1−85) is homologous to Atox1, the chaperone for Wilson and Menkes disease proteins, and contains the metal binding motif MXCXXC (MTCQSC in hCCS), common among copper chaperones. DI is thought to sequester copper under metal starvation conditions. Domain II (DII, residues 86−234) is the SOD-like domain and has been hypothesized to play a role in SOD recognition. With the exception of mammalian species, SOD metal-binding sites are not conserved in the DII region of most known forms of CCS. Domain III (DIII, residues 235−274) is a short C-terminal tail that contains the metal-binding motif CXC (CSC in hCCS) and is thought to be the structural element that delivers copper to SOD (*23*, *30*).

Previous work on the yeast CCS showed that apo-yCCS is a monomer while Cu-yCCS exists in a monomer/dimer equilibrium (*30*). A crystal structure of yCCS showed a homodimer, with a dimer interface in DII similar to that of the SOD dimer interface (*31*). Unfortunately, this structure was uninformative as to the coordination of bound copper ions, since the DI metal-binding motif was present as a disulfide, while DIII was disordered. Further work with yCCS and H48F ySOD, a mutant that is unable to bind copper, showed that the yCCS and the mutant SOD formed a 48 kDa species upon gel filtration, which is the mass expected for the heterodimer (*24*). Crystallization of the yCCS−H48FSOD complex showed a heterodimer associated via the same residues used to form the dimer interfaces of the individual homodimers of SOD and DII of the CCS, but again, no metal ions were bound in the structure (*32*). The structure also showed a disulfide bond between yCCS Cys229 (Cys244 in hCCS) and SOD Cys57. In wild-type SOD, Cys57 forms a disulfide bond in the metal-binding loop of the Cu and Zn site, and it has been further suggested that CCS may catalyze the formation of this critical disulfide bond in SOD (*33*−*35*).

Unlike many other species, human CCS (hCCS) retains most of the SOD metal-binding residues in DII with the exception of one of the copper-binding histidines (H120 in SOD) which has changed to an aspartate residue (D201) in CCS. A truncated form of the protein containing domain II only has been studied by X-ray crystallography, and shows a homodimer with one zinc bound by the conserved metal ligands in each monomer (*36*). Notwithstanding, the absence of copper bound in any of the structures emphasizes how little is known about the coordination of the Cu(I) metal sites of the protein. Our previously reported X-ray absorption spectroscopic (XAS) data of fully reduced hCCS suggested the presence of a copper cluster, where each copper was coordinated by three cysteinyl S scatterers at 2.24 Å with a prominent Cu−Cu interaction at 2.73 Å (*37*). We proposed a Cu(I) binding site composed of a dinuclear μ_2-cysteinyl-bridged cluster formed between the metal-binding cysteines in DI and DIII. The ability of DI and DIII to interact in this way was reinforced by a study of Co(II) binding to tomato CCS suggesting that Co(II) bound in a distorted tetrahedral environment to the cysteine ligands of both domains (*38*).

To continue our work on hCCS, we report here Zn-EXAFS of the wild-type protein as well as Cu-EXAFS on a variety of mutants of hCCS (C22S, C244S, C22/25S, and C244/246S). Also, we measured the ability of WT hCCS and its mutants to transfer copper to hSOD. This work showed that while zinc binding remained unchanged from wild type to mutant, the copper binding changed dramatically in the double mutants. The changes in the copper environment suggested that the two copper ions are bound to two different sites within the hCCS protein. Site-directed mutagenesis of the DI and DIII cysteine residues suggests that one Cu(I) is bound to DI in a three-coordinate geometry composed of two cysteines and one exogenous ligand, while a second copper forms an intermolecular cluster between DIII of two different hCCS monomers.

EXPERIMENTAL PROCEDURES

Cloning, Expression, and Purification of hCCS and rSOD. hCCS cDNA was PCR-amplified from a human fetal brain cDNA library by use of primers at the 5′ and 3′ terminus (5′-GGCCTACCGCGGTATGGCGACGAAGG-3′ and 5′-CCAAGGGAATGTTCCATGGGCGATC-3′). The cDNA was cloned into the pMAL-c2X expression vector (New England Biolabs) by use of restriction sites *Eco*RI and *Hin*dIII introduced in the 5′ and 3′ PCR primers, respectively (*39*). Mutagenesis was carried out by an overlap extension approach. Primers were designed to substitute single cysteines with serines. Each single amino acid substitution was cloned into the pMAL-c2X vector and expressed as above. Additionally, two double serine mutants were also con-

structed and expressed. All expression constructs were confirmed by automated DNA sequence analysis.

The fusion protein contained an N-terminal maltose binding protein (MBP) tag (for purification on an amylose resin) of 48 kDa containing no metal binding sites, connected to the 29 kDa hCCS construct by a 3 kDa arginine-rich linker legion. The expression was designed to start at the ATG start codon in MBP and stop at the TGA stop codon after the C-terminus of hCCS. The full expression is 666 amino acids long.

The maltose binding protein−hCCS fusion protein (MBP−hCCS) was expressed in the *Escherichia coli* strain BL21 (DE3) (Novagen) (BL21) after induction with isopropyl thio-β-D-galactoside (IPTG) in the presence of 500 μM $CuSO_4$ and 500 μM $ZnSO_4$. The cells were lysed with a French pressure cell press (SLM-Aminco). The MBP−CCS fusion protein was purified from the soluble portion on an amylose column. The amylose resin (New England Biolabs) was packed into an XK 16/20 column with an AK 16 adaptor (Amersham Pharmacia Biotech). Buffer flow into the column was controlled with a peristaltic pump, and the hCCS fraction leaving the column was monitored with a UV-1 single-path monitor (Amersham Pharmacia Biotech). When necessary, the protein was concentrated with an Amicon Centricon ultrafiltration cell.

Recombinant human SOD (rSOD) was cloned as a *Sap*I−*Nde*I fragment generated by PCR amplification of a cDNA clone obtained from Genome Systems (GB Accession Number AA702004). PCR primers that contained the restriction sites *Sap*I (5′) and *Nde*I (3′) were used to amplify SOD cDNA. This PCR fragment was cloned into the intein pTXB-1 vector from New England Biolabs.

Recombinant human SOD was expressed in the *E. coli* strain ER2566 (Novagen) after induction with IPTG in the presence of 500 μM $ZnSO_4$. The cells were lysed with a French pressure cell press. Recombinant human SOD was purified from the soluble portion with a chitin column. The chitin beads (New England Biolabs) were packed into an XK 16/20 column with an AK 16 adaptor and washed with 10 volumes of 50 mM sodium phosphate buffer and 500 mM sodium chloride, pH 7.2 (column buffer). The soluble portion was diluted three times with column buffer and run over the chitin column. The column was washed with another 10 volumes of column buffer followed by 3 volumes of column buffer plus 5 mM 2-mercaptoethanesulfonate (cleavage buffer). One volume of cleavage buffer was then added to the column and allowed to sit overnight. The cleavage buffer was removed from the column as the first fraction and another 3 volumes of cleavage buffer were added to the column. All of the fractions were saved and combined. When necessary, the protein was concentrated with an Amicon Centricon ultrafiltration cell. The purified protein contained one Zn ion per monomer, and was presumed to be the E,Zn form. Fully metal-loaded Cu,Zn-SOD was obtained by adding excess $CuSO_4$ to the E,Zn-SOD followed by exhaustive dialysis against Cu-free column buffer.

Protein and Metal Analysis. Protein concentration was measured by Bradford and bicinchoninic acid-based assays (Sigma). The accuracy of the Bradford assay was tested by comparison to amino acid concentration analysis performed by the AAA Service Laboratory, Boring, OR. It was found that a correction factor of 1.05 was necessary when protein was determined by the Bradford method with bovine serum albumin as standard. Copper was measured by bicinchoninic acid-based assay (Sigma) or by atomic absorption/emission spectrophotometry on a Varian-Techron AA-5 atomic absorption spectrophotometer or on a Perkin-Elmer Optima 2000 DV inductively coupled plasma optical emission spectrophotometer (ICP OES). The oxidation state of the copper was determined by electron paramagnetic resonance spectroscopy (EPR) versus a Cu(II)−ethylenediaminetetraacetic acid (EDTA) standard on a Bruker Elexys 500 EPR spectrometer. The zinc concentration was measured by atomic absorption spectroscopy and ICP OES spectroscopy.

SOD Reconstitution Assays. The ability of CCS to transfer copper to SOD was investigated by incubation of CCS with E,Zn-SOD for 15 min at 37 °C in a buffer of 50 mM sodium phosphate containing 10 μM bathocuproin sulfonate and 10 μM EDTA at pH 7.8. The activity of the SOD was then measured by its ability to inhibit the reduction of cytochrome *c* by superoxide generated by the xanthine/xanthine oxidase reaction (*27*).

XAS Data Collection and Analysis. Cu K-edge (8.9 keV) and Zn K-edge (9.6 keV) extended X-ray absorption fine structure (EXAFS) and X-ray absorption near edge structure (XANES) data for the hCCS and the hCCS mutants were collected at the Stanford Synchrotron Radiation Laboratory operating at 3 GeV with currents between 100 and 50 mA. All samples were measured on beam line 9-3 by use of a Si[220] monochromator and a Rh-coated mirror upstream of the monochromator with a 13 keV energy cutoff to reject harmonics. A second Rh mirror downstream of the monochromator was used to focus the beam. Data were collected in fluorescence mode on a high-count-rate Canberra 30-element Ge array detector with maximum count rates below 120 kHz. A 6 μ Z-1 metal oxide (Ni, Cu) filter and Soller slit assembly were placed in front of the detector to reduce the elastic scatter peak. Nine scans of a sample containing only sample buffer (20 mM $NaPO_4$ and 500 mM NaCl, pH 7.0) were collected at each absorption edge, averaged, and subtracted from the averaged data for the protein samples to remove Z-1 K_β fluorescence and produce a flat pre-edge baseline. This procedure allowed data with an excellent signal-to-noise ratio to be collected down to 100 μM total copper in the sample. The samples (70 μL) were measured as aqueous glasses (>20% ethylene glycol) at 15 K. Energy calibration was achieved by reference to the first inflection point of a copper foil (8980.3 eV) for Cu K-edges and a zinc foil (9660.0 eV) for Zn K-edges, placed between the second and third ionization chamber. Data reduction and background subtraction were performed with the program modules of EXAFSPAK (*40*). Data from each detector channel were inspected for glitches or drop-outs before inclusion in the final average. Spectral simulation was carried out with the program EXCURVE 9.2 (*41*−*44*) as previously described (*37*, *45*) or with the OPT module of EXAFSPAK with the theoretical phase shifts and amplitude functions calculated by FEFF 8.0 (*46*). Both programs gave equivalent results.

RESULTS

Human CCS was expressed as a maltose binding protein fusion. Wild-type hCCS and four mutant proteins carrying

Table 1: Metal Binding Properties and Metal Transfer Activities of hCCS and Its Mutants

	Cu/P	N[a]	Zn/P	N[a]	% activity[b]	N[a]
wild type	1.85 ± 0.10	12	0.91 ± 0.08	9	91.1 ± 5.3	12
C22S	1.60 ± 0.28	5	0.72 ± 0.13	5	82.8 ± 3.4	5
C244S	1.66 ± 0.10	5	0.87 ± 0.04	5	87.0 ± 6.1	5
C22/25S	0.91 ± 0.12	4	0.86 ± 0.07	4	75.5 ± 4.4	4
C244/246S	0.92 ± 0.10	5	0.95 ± 0.08	5	15.9 ± 4.0	2

[a] N represents the number of determinations of the parameter to the left in the table. [b] Percent maximum activity as compared to Cu,Zn-SOD.

Cys to Ser mutations on the putative metal-binding cysteine residue of the DI CXXC and DIII CXC motifs were purified on amylose affinity columns in yields between 15 and 30 mg/L of culture. The presence of the N-terminal maltose binding protein purification tag did not affect either the activity or spectroscopic properties of the WT protein, since an untagged hCCS construct expressed in an intein vector displayed identical properties (data not shown).

Metal Binding. WT hCCS expressed in the presence of 500 μM $CuSO_4$ and 500 μM $ZnSO_4$ purified with 1.85 Cu(I) and 0.91 Zn atoms/protein (Table 1). This was compared to previous methods of expression (*37*) where zinc was not included during induction and the protein purified with >3 copper ions, a significant amount of which was in the Cu(II) form. In these earlier studies, reduction with dithionite followed by exhaustive dialysis was necessary to remove the "adventitious" cupric ions, after which the protein bound 2 Cu(I) ions/protein molecule. In the present study, addition of zinc to the induction medium eliminated the need for any postpurification reduction and produced a protein that purified with 2 coppers/hCCS (see Table 1).

The single mutants, C22S and C244S, were found to have similar metal-binding capacities to the WT protein when expressed under the same conditions. C22S purified with 1.60 Cu and 0.72 Zn, while C244S contained 1.66 Cu and 0.87 Zn/protein. The most noticeable difference was observed with the double mutants, C22/25S and C244/246S. In both of these mutants zinc binding remained unchanged but copper binding dropped to 1 Cu/protein. C22/25S had 0.91 Cu and 0.86 Zn/protein, and C244/246S contained 0.92 Cu and 0.95 Zn/protein.

Activity. The activity of CCS is expressed as the increase in SOD activity (relative to E,Zn-SOD) after incubation of SOD with hCCS at 37 °C for 15 min, where a unit of SOD is defined as the amount of SOD needed to reduce by 50% the rate of reduction of cytochrome *c* by xanthine/xanthine oxidase under standard conditions (*27*). To test the effect on activity of varying the CCS:SOD ratio, the ratio of hCCS to SOD in the incubation mixture was increased from 0 to 3.0 CCS:SOD in 10 aliquots. The activity maximum was reached at a ratio of 1 hCCS:1 SOD (data not shown). At this ratio, WT CCS was able to restore 1276 units/mg to E,Zn-SOD (Table 1). When E,Zn-SOD was dialyzed against free cupric ion as described under Experimental Procedures, 1400 units of activity were recovered. Thus incubation with CCS was able to restore 91% of SOD activity. When the time of incubation of hCCS with SOD was varied, SOD reached its maximum activity in less than 5 min (the time necessary to complete the assay measurement).

When the DI single mutant C22S was incubated with E,Zn-SOD under standard conditions it gave an activity 33% of WT CCS, at a concentration ratio of 1:1 CCS:SOD and an incubation time of 15 min. Increasing the concentration of C22S CCS increased the activity until a maximum was reached at an 8:1 ratio of C22S CCS to E,Zn-SOD. Under these conditions, incubation for 15 min gave an SOD activity of 1056 units/mg, 83% of WT activity. Keeping the ratio of C22S CCS and E,Zn-SOD at 1:1 and increasing the incubation time had no effect on maximum activity.

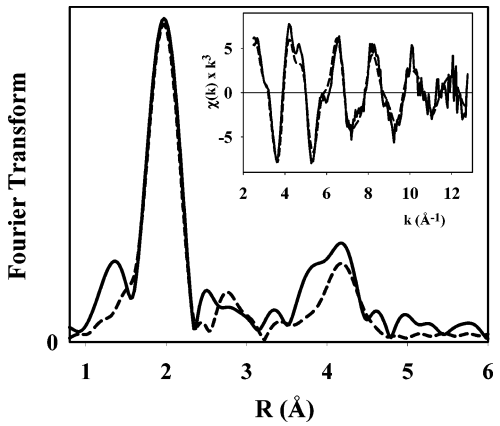

FIGURE 2: Experimental (—) and simulated (---) Fourier transform and EXAFS (inset) for the Zn K-XAS of wild-type hCCS. Parameters used for the simulation are listed in Table 2.

When the DIII single mutant C244S was incubated with E,Zn-SOD under standard conditions, it showed an activity 31% that of WT hCCS. Increased incubation time had little effect on the activity of C244S CCS, but increasing the concentration ratio of the C244S mutant 8 times in the incubation mixture increased the activity of SOD to about 87% that of wild type (1110 units/mg).

The DI double mutant, C22/25S, reduced the SOD activity to 76% that of wild-type CCS with an activity of 964 units/mg. Both increasing time and concentration had little effect on the activity of this mutant. On the other hand, the DIII double mutant, C244/246S, was only able to restore 16% of the activity of the wild-type protein. Neither increased concentration nor increased incubation time could rescue the activity of this DIII mutant.

Zn K-Edge XAS. Figure 2 shows experimental and simulated Zn-EXAFS of the Zn center in WT hCCS. The data fit well to a 4 O/N shell at 1.983 Å with histidine multiple scattering from 3 ± 1 histidines (Table 2, fit A). The fit is improved by including an additional low *Z* scatterer, suggesting that in contrast to the SOD homologue, the Zn center of CCS may recruit an additional ligand. The improved fit (Table 2, fit B) has a more reasonable Debye-Waller (DW) value for the nonhistidine shell. The data are similar to spectra reported previously for the Zn center in Cu/Zn-SOD (*28*, *47*, *48*) and most likely represent a three histidine/one aspartate coordination environment as expected from the crystal structures of hCCS DII (*36*).

Cu K-Edge XAS. The Cu XAS of the WT protein (Figure 3) has an edge jump at 8980.2 eV with an edge feature at 8983.3 eV. The position of the edge jump is typical of Cu(I) species (confirmed by the absence of EPR signal). The energy of the edge jump and the 8983 eV edge feature is invariant from the WT protein to the mutants, but some variation in the intensity of the 8983 eV transition was

Table 2: Fits Obtained to the Zn-EXAFS of the Cu(I)-Loaded hCCS by Curve-Fitting with the Program EXCURV 9.2

Zn−His[a]			Zn−O/N			
no.[b]	R[c] (Å)	DW[d] (Å^2)	no.[b]	R[c] (Å)	DW[d] (Å^2)	E_0
Fit A, $F = 0.702$[e]						
3 N_α	1.983	0.0025	1	2.011	0.0005	−5.83
3 C_β	2.81	0.0060				
3 C_β	2.99	0.0060				
3 $N\gamma$	4.18	0.0060				
3 $C\gamma$	4.22	0.0060				
Fit B, $F = 0.549$[e]						
3 N_α	1.958	0.0030	2	2.027	0.0015	−6.10
3 C_β	3.00	0.0050				
3 C_β	2.85	0.0050				
3 $N\gamma$	4.19	0.0075				
3 $C\gamma$	4.22	0.0075				

[a] Fits modeled histidine coordination by an imidazole ring, which included all single and multiple scattering contributions from the first shell (N1 = N_α), second shell (C2/C5 = C_β) and third shell (C3/N4 = C_γ/N_γ) atoms, respectively. The histidine ligands were modeled by use of idealized imidazole ring geometry with Zn−N1−C2/C5 angles = ±127° and Zn−N1−C3/N4 angles = ±163°. [b] Coordination numbers are generally considered accurate to ±25%. [c] In any one fit, the statistical error in first-shell bond lengths is ±0.005 Å. (For outer-shell bond lengths the error is larger, ±0.05 and 0.2 Å for the C_β and C_γ/N_γ shells respectively.) When errors due to imperfect background subtraction, phase-shift calculations, and noise in the data are compounded, the actual error in first-shell distances is probably closer to ±0.02 Å. [d] The DW factors are listed as σ^2 values rather than the $2\sigma^2$ values output by the EXCURVE program. [e] F is a least-squares fitting parameter defined as $F^2 = (1/N)\sum_{i=1}^{N} k^6$ (data − model)^2.

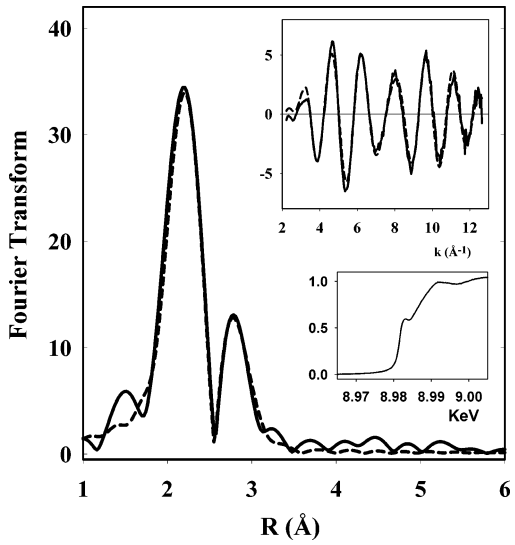

FIGURE 3: Experimental (—) and simulated (---) Fourier transform and EXAFS (top inset) for the Cu K-XAS of wild-type hCCS. Parameters used for the simulation are listed in Table 3, fit A. Bottom inset: XANES region of the XAS spectrum.

observed (decreasing in the order WT > C22/25S > C22S > C244S > C244/246S).

Previous EXAFS studies on the Cu sites of CCS (*37*) isolated from cells grown without added zinc showed a mixed environment with both copper−sulfur and copper−histidine coordination. Reduction with either sodium dithionite or dithiothreitol followed by dialysis to remove the reductant resulted in loss of the copper−histidine component and a decrease in Cu:CCS stoichiometry from 3.5 to 2 coppers/protein. We interpreted these observations as evidence that copper could bind to histidine residues in DII, at either of

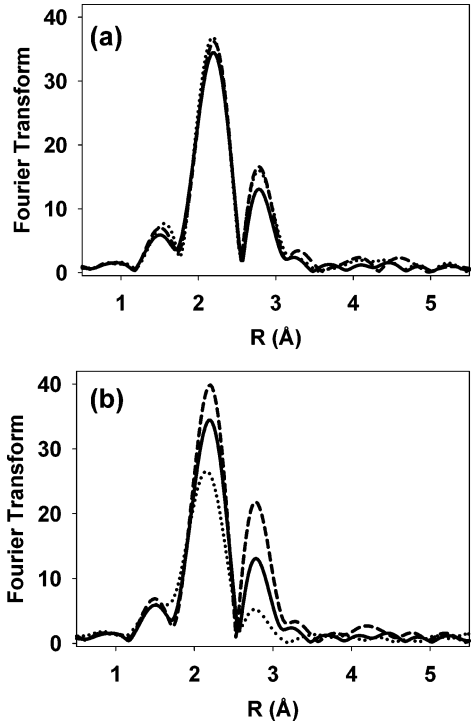

FIGURE 4: Comparison of the experimental Fourier transforms of single and double mutants of hCCS. (a) Wild type (—), C22S (---), and C244S (···); (b) wild type (—), C22/25S (---), and C244/246S (···).

the sites that resembled the copper and zinc sites of SOD. In the present study, growing the cells in the presence of 500 μM Zn^{2+} produced a protein with 1 Zn and 2 Cu ions/CCS. Figure 3 shows the Cu K-EXAFS of the two-copper protein. The characteristic beat patterns of imidazole in the $k = 3-5$ Å^{-1} (*45*) are absent, and the spectrum is dominated by intense scattering from Cu−S interactions. Simulation of the data by curve-fitting protocols was carried out with the two-shell model obtained previously, viz., 3 Cu−S at ∼2.26 Å and 1 Cu−Cu at ∼2.7 Å. Good fits were obtained with the first shell as a sulfur scatterer at 2.256 Å and the second shell consisting of a copper at 2.712 Å (Table 2, fit A).

Despite the mutation, the Cu-EXAFS of the single mutants remained comparable to that of the wild-type protein. Figure 4a compares the experimental (phase-corrected) Fourier transforms of WT protein and the two single mutants. In the C22S mutant, an excellent fit to the EXAFS was obtained with parameters almost identical to WT (Table 2, fit B). It was also possible to achieve a comparable fit by reducing the sulfur shell to $N = 2.5$ and adding 0.5 oxygen at 2.043 Å (Table 2, fit C). The C244S mutant Cu-EXAFS was almost identical to that of the C22S mutant. No significant changes were observed in the Cu environment from that of WT, and the C244S data could be adequately simulated with parameters identical to those obtained for the WT simulation within experimental error (Table 2, fit E). Again, a slightly better fit was obtained when 0.5 O scatterer was included at 2.052 Å and the Cu−S shell occupancy was reduced to 2.5 (Table 2, fit F). It should be noted that the Cu−O and Cu−S contributions to the EXAFS are almost perfectly in phase over a significant part of the data range, such that the Cu−O and Cu−S shell occupancy is highly correlated. For this reason, the data do not easily distinguish between fits that

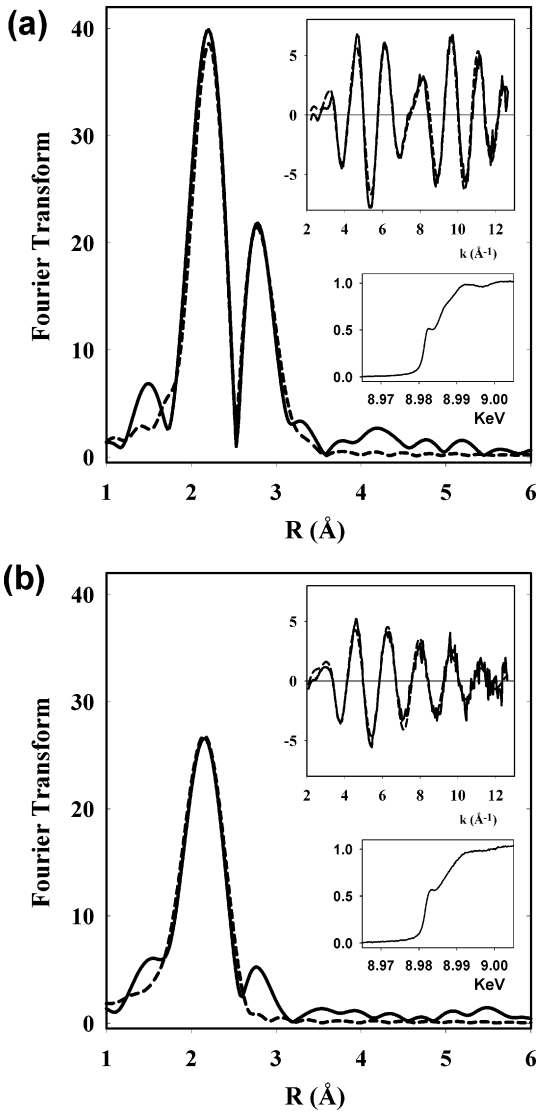

FIGURE 5: Curve fitting of the EXAFS of double mutants C22/25S and C244/246S. Experimental (—) and simulated (---) Fourier transform and EXAFS (top inset) for (a) C22/25S hCCS and (b) C244/246S hCCS are shown. Parameters used for the simulation are listed in Table 3, fits J and L, respectively. Bottom insets show the XANES region of the spectra.

include Cu−O contributions from those containing only Cu−S scatterers.

The DI double mutant (C22/25S) was also found to have a large second-shell feature. A good fit was obtained for its Cu-EXAFS with a first shell of three sulfur atoms at 2.259 Å and a second shell of a copper at 2.712 Å. Experimental and simulated EXAFS and Fourier transforms for this mutant are shown in Figure 5a. The largest difference between the wild type and C22/25S Cu-EXAFS was a significant increase in the intensity of the Cu−Cu peak, which was simulated by a decrease in the DW (σ^2) factor of the Cu−Cu shell from 0.0045 Å^2 to 0.0025 Å^2 (Table 2, fit I). The near 50% decrease in the Cu−Cu DW prompted us to explore fits that included two Cu scatterers at the 2.7 Å distance. For the C22/C25S double mutant, two copper scatterers fitted better than one, leading to a decrease in F from 0.475 to 0.382 (Table 3, fit J) with a Cu−Cu DW which now matched that observed for the WT protein. It was also found that the C22S and C244S single mutant data could be fit with more than one Cu scatterer at 2.7 Å (Table 3, fits D and G), but in these cases, no improvement in *F* was observed. This may signal that the cluster which gives rise to the second-shell Cu−Cu interaction in the C22/C25S DI double mutant may involve a nuclearity greater than 2.

The DIII double mutant C244/246S was the only mutant to show a loss of the second-shell feature. The Fourier transform of C244/246S (Figure 4b) shows a single peak centered around 2.2 Å with a reduced intensity relative to WT, and a small shift in the peak maximum to lower *R*. These changes could represent either a lower coordination number [due to Cu(I) binding to the two Cys residues of DI only] or the presence of a low *Z* scatterer accompanying Cu−S ligation. The similarity in the intensity of the 8983 eV 1s → 4p transition to WT and to the C22/C25S mutant (Figures 3 and 5a) indicates that the C244/C246S is most likely 3-coordinate, since 2-coordinate sites give rise to more intense 8983 transitions (*49*−*52*). The EXAFS spectrum is well fit by two sulfur scatterers at 2.259 Å and one oxygen at 2.012 Å (Table 2, fit L, and Figure 5b). A comparable fit was obtained with three sulfur scatterers at 2.229 Å (Table 3, fit K), but this fit required a higher Cu−S DW factor than for any other mutant and showed a decreased Cu−S distance. Although a decreased Cu−S distance would be consistent with 2-coordination, fits to the EXAFS data with just two Cu−S interactions were unacceptable. Therefore, it seems probable that the C244/246S DIII double mutant contains a single Cu(I) coordinated to the Cys residues of the CXXC DI motif with a further interaction with an exogenous O/N (solvent) ligand.

DISCUSSION

In the present paper, we present new results on copper binding, metal transfer activity, and spectroscopic characterization of site-directed mutants of the copper chaperone for superoxide dismutase. Since the published crystal structures do not contain bound copper, information in the literature on the copper coordination has relied on EXAFS spectroscopy (*37*) or been inferred indirectly from UV/vis studies on Co(II)-bound forms of CCS (*38*). These studies have suggested that pairs of Cys residues—C22 and C25 in domain I and C244 and C246 in domain III—act as ligands to Cu(I) in the copper-loaded WT CCS. To provide a more detailed picture of the copper coordination in hCCS, we embarked on studies of two Cys to Ser single mutants, C22S and C244S, where a single Cys residue in each of the putative Cu(I) binding sites was mutated. We also studied two double mutants, C22/25S and C244/246S, in which both Cys residues at each site were mutated to Ser. All of the mutants were studied by X-ray absorption spectroscopy at the copper and zinc K-edges, and the structures were compared with those of the Cu and Zn centers in the WT protein.

In our earlier studies, in which hCCS was expressed without supplementation of the medium with zinc, we observed copper binding ratios in excess of 3 Cu/protein, a proportion of which was shown by EPR to be oxidized Cu(II) (*37*). Since the hCCS protein contains vestigial SOD-like metal binding sites in DII and has been shown by crystallography to bind Zn (*36*), we postulated that the extra copper was bound within the DII metal binding sites. Dialysis against either sodium dithionite or DTT decreased the copper

Table 3: Fits Obtained to the Cu-EXAFS of Wild-Type Cu(I) hCCS and Its Cys to Ser Mutants with the Program EXCURV 9.2

		Cu−S			Cu−O			Cu−Cu			
fit	F[a]	no.[b]	R[c] (Å)	DW[d] (Å^2)	no.[b]	R[c] (Å)	DW[d] (Å^2)	no.[b]	R[c] (Å)	DW[d] (Å^2)	E_0
					Wild Type						
A	0.332	3	2.256	0.0054				1	2.712	0.0045	−4.78
					C22S						
B	0.524	3	2.260	0.0050				1	2.704	0.0035	−3.92
C	0.510	2.5	2.270	0.0044	0.5	2.043	0.0020	1	2.712	0.0035	−5.96
D	0.480	2.5	2.270	0.0040	0.5	2.035	0.0020	2	2.716	0.0080	−5.98
					C244S						
E	0.548	3	2.251	0.0050				1	2.706	0.0048	−3.77
F	0.548	2.5	2.260	0.0047	0.5	2.052	0.0020	1	2.713	0.0035	−5.84
G	0.456	2.5	2.260	0.0043	0.5	2.045	0.0020	2	2.717	0.0080	−6.00
					C22/25S						
H	0.475	3	2.259	0.0049				1	2.712	0.0025	−4.48
J	0.382	3	2.260	0.0040				2	2.716	0.0055	−4.75
					C244/246S						
K	0.574	3	2.229	0.0074							
L	0.568	2	2.259	0.0056	1	2.012	0.0035				

[a] F is a least-squares fitting parameter defined as $F^2 = (1/N)\sum_{i=1}^{N} k^6(\text{data} - \text{model})^2$. [b] Coordination numbers are generally considered accurate to ±25%. [c] In any one fit, the statistical error in bond lengths is ±0.005 Å. However, when errors due to imperfect background subtraction, phase-shift calculations, and noise in the data are compounded, the actual error is probably closer to ±0.02 Å. [d] The DW factors are listed as σ^2 values rather than the $2\sigma^2$ values output by the EXCURVE program.

to protein stoichiometry to 2:1 and resulted in all the copper bound in the Cu(I) state. In the present study, we have shown that simple addition of 500 μM zinc + 500 μM copper as divalent metal salts to the growth medium is sufficient to populate the Zn site in DII and produces a WT protein with 1 Zn and 2 Cu atoms/monomer. This contrasts with other work (*23*) where 1 mM $CuSO_4$ supplementation of the medium led to protein with copper binding stoichiometries in the range 1−1.2.

Single Cys to Ser mutations, as represented by C22S and C244S, did little to affect the metal binding ratios of hCCS. Both mutants still showed approximately 2 Cu(I) ions and 1 Zn ion/protein. The double mutants C22/25S and C244/246S, on the other hand, showed copper binding stoichiometries close to 1:1. Therefore, to perturb the metal binding of hCCS, both Cys residues of the domain I or domain III metal binding sites had to be eliminated.

EXAFS data at the Zn edge is consistent with the presence of a single Zn bound to hCCS. Simulations imply a Zn site composed of low-Z (O/N) scatterers, with 3−4 histidine residues, and are fully consistent with Zn binding at the SOD-like metal binding site in domain II. This finding is in agreement with the crystal structure of the DII-truncation hCCS (*36*). The number of bound Zn atoms changes little between WT and the mutants. The Zn-EXAFS of the mutants also show that the zinc is most likely bound in the conserved SOD binding site and is insensitive to mutation of the copper binding ligands. The role of Zn in the structure and mechanism of hCCS was not further explored in this study.

The in vivo copper loading protocol developed in this study allowed us to examine the Cu EXAFS of hCCS with 2:1 stoichiometry without the need for reductive removal of metal bound to domain II. The XANES of the WT protein was typical of trigonal copper(I)−thiolate species (*51*, *52*), and the absence of an EPR signal also supports the Cu(I) assignment. No 8979 eV feature due to the quadrupole-allowed 1s → 3d transition was observed. All of the spectra showed an edge feature at 8983 eV, which is characteristic of a Cu(I) species and has been assigned to a 1s → 4p transition (*49*−*52*). EXAFS analysis of the WT protein gave metrical parameters closely similar to those reported previously. The FT showed a strong outer-shell feature that we and others have attributed to a Cu−Cu interaction within a copper cluster. The simulations gave appropriate distances for both the Cu−S and the Cu−Cu shells (*51*, *52*).

In our previous study of the WT protein, we suggested that the copper cluster was intramolecular and was formed from a pair of trigonal Cu(I) centers in both DI and DIII, with one terminal and two bridging cysteines on each copper. EXAFS analysis of the mutant proteins has shed further light on the copper coordination in each domain and the identity of the copper cluster. Cu K-edge EXAFS data for the DI and DIII single mutants (C22S and C244S) were similar to those for the WT, and the parameters deduced for the WT gave a very good fit to both single mutant spectra. This shows that the single mutation of a Cys to Ser is not enough to disrupt the copper−thiolate cluster, as observed previously by Winge and co-workers in studies of the COX17 copper chaperone (*18*). The data appear consistent with O from serine replacing one or more S scatterers in the cluster, as entirely equivalent fits were obtained if one S was replaced by O (see Table 2). Thus, the Cys to Ser single mutants are uninformative with respect to interpreting the coordination chemistry.

The double mutants, on the other hand, showed much more interesting behavior. Removal of the DI binding sites, as in the C22/25S mutant, showed an EXAFS spectrum exactly as expected for a fully trigonal copper−thiolate cluster. This result argues that, in this mutant at least, the cluster cannot be intramolecular but must be formed between two DIII CXC binding sites within an hCCS dimer. Further, the only mutant to show a loss of the cluster was the DIII double mutant, C244/246S. This showed a much simplified EXAFS and Fourier transform that lacked the outer-shell Cu−Cu feature and could be fit by a simple 3-coordinate site with two sulfur and one oxygen scatterers. Here the fit was improved by

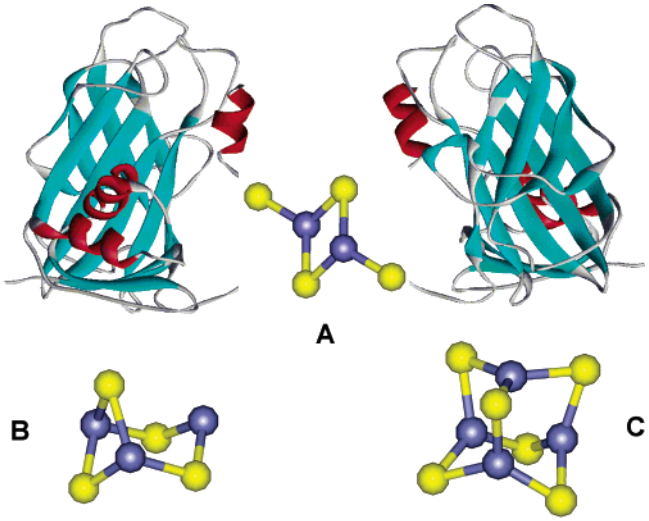

FIGURE 6: Possible cluster structures for the DIII−DIII interaction in hCCS. (a) Bis-cysteine bridged dinuclear cluster. (b) Trinuclear cluster based on a Cu_3S_3 hexagonal ring with one additional bridging cysteine. (c) Cu_4S_6 tetranuclear cluster composed of three fused Cu_3S_3 hexagonal rings.

the addition of one oxygen to the first shell, as would be expected for an isolated 3-coordinate DI Cu(I) center with two Cys residues and one solvent as ligands. The Cu−S distances of 2.259 Å agree with previous data on trigonal copper complexes. Taken together, these data strongly suggest that the C22/C25S double mutant binds Cu(I) in a structure composed of an hCCS dimeric or tetrameric structure in which a cluster forms at the interface of two DIII polypeptides, leaving the two DI metal sites monomeric. The data do not inform as to whether the WT and single C → S mutants bind Cu(I) in a similar intermolecular cluster, in an intramolecular DI−DIII cluster as proposed previously, or in an equilibrium between both.

EXAFS analysis gives a number of important clues to the structural identity of cuprous thiolate clusters (*51*, *52*). Cu−S bond length and 8983 eV peak intensity are useful indicators of coordination number, while the Cu−Cu distance and intensity provide information on cluster nuclearity. Our data provide strong support for trigonal Cu(I) centers, with one or more Cu−Cu interactions within the cluster. Possible cluster models are shown in Figure 6. The simplest case is the dinuclear cluster shown in Figure 6a, with each Cu(I) bound by one terminal and two bridging cysteine ligands, previously suggested by us in WT CCS and by others in Cox 11 (*14*, *15*). However, a search of the Cambridge database reveals no examples of a dinuclear trigonal Cu(I) cluster in the inorganic literature [all such clusters have 4-coordinate Cu(I) geometry], and examples with other metals (Fe, Zn) have longer M−M bond lengths (3.1−4.0 Å). Cu(I)−Cu(I) interactions of 2.7 Å are exhibited typically in clusters such as those depicted in Figure 6b,c, which are built from Cu_3S_3 fused rings. Our finding that the DIII−DIII cluster fits better to nuclearities greater than 1 may provide evidence for a more complex cluster geometry. Further work will be required to investigate this possibility.

The WT protein was fully capable of activating SOD as previously reported (*23*). When SOD was titrated with hCCS, maximum activity was observed when the ratio of hCCS to SOD was 1:1. If both coppers from CCS were transferring to SOD, the expected ratio would be 1 hCCS:2 SOD since there are two coppers per hCCS monomer but only one copper per SOD monomer. This implies that although CCS binds two coppers, it only transfers one of those coppers to SOD. The only mutant to lose activity was the DIII double mutant, C244/246S, which agrees well with other reports in the literature that DIII is the site of transfer of copper to SOD (*23*, *30*, *35*). The DI double mutant, C22/25S, retained activity but at reduced levels and was not rescued with increased time of incubation or an increase of hCCS to SOD ratio. It is possible that DI acts to sequester copper from other protein partners or from the intracellular matrix and is not directly involved in transfer to SOD. Alternatively, it could play some important structural or regulatory role.

The most puzzling results are those of the single mutants, C22S and C244S, which show very similar activity profiles to one another, even though they contain mutations in different domains. Recent studies have suggested a new and intriguing functional role for the CCS chaperone: Brown et al. (*34*) showed that activation of SOD by hCCS required the presence of either O_2 or superoxide, while Furukawa et al. (*35*) demonstrated a clear role for yCCS in the formation of the essential ySOD disulfide. These studies have led to a novel mechanism for O_2-dependent posttranslational modification of SOD by CCS involving initial oxidative disulfide formation within a heterodimeric CCS−SOD complex, in which thiol and Cu(I) oxidation proceed at the CCS DIII SOD interface. It is suggested that the products of the initial CCS−SOD interaction undergo further processing, involving copper transfer as Cu(II) and disulfide isomerization to generate the SOD disulfide.

The crystallographically observed heterodisulfide between yCCS C229 and SOD C57 offered powerful supporting evidence in favor of this new mechanism (*32*). However, in the present study, mutation of the homologous cysteine (C244) to serine did not eliminate activity; rather it induced an altered activity profile that could be fully rescued by increasing the CCS concentration. This result suggests that the mechanism must be more complex than simple oxidative heterodisulfide formation, which is expected to be turned off if one of the participating thiols is replaced by OH. It is possible that another cysteine residue (C246 or possibly C144 in DII) could replace C244 in this step, but that seems unlikely unless the docking between the two proteins is conformationally mobile. Given the evidence for cluster formation between two DIII segments of isolated CCS, it is interesting to speculate that a similar cluster might form between the cysteines of the CCS DIII and the SOD thiols destined for disulfide formation. Indeed, such clusters appear to be increasingly common in copper chaperone systems and have been proposed as intermolecular cross-links in the dimeric form of the cytochrome *c* oxidase assembly protein COX11 (*14*, *15*).

The altered activity of the CCS single mutants could be explained by other mechanisms. Our EXAFS data are consistent with the possibility that hCCS can form two types of clusters, an inactive intramolecular complex between DI and DIII and an active intermolecular complex between two DIII metal-binding regions. If the Cys to Ser single mutants were unable to convert any DI−DIII complex into a DIII−DIII complex, then only the percentage of the population of hCCS that was in the DIII−DIII complex form would be

active. The part of the population stuck in the unproductive DI−DIII form would be inactive. The only way to rescue the activity would be to increase the concentration of hCCS until the concentration of the hCCS in the DIII−DIII form was equal to that of the concentration of SOD.

Although the interpretation of the Cys to Ser single mutations is still unclear, our results point to a clear role for the DIII Cu(I) complex in SOD activation. Present data also support cluster formation in the active CCS−SOD complex, since a monomeric Cu(I) DIII complex is unlikely to be stabilized by a single Cys residue. Further work is underway to probe these and other aspects of the CCS−SOD mechanism.

ACKNOWLEDGMENT

We thank Mary Mayfield Gambill for help with construction and expression of mutant proteins. We gratefully acknowledge the use of facilities at the Stanford Synchrotron Radiation Laboratory.

REFERENCES

1. Fridovich, I. (1989) Superoxide dismutases. An adaptation to a paramagnetic gas, *J. Biol. Chem. 264*, 7761−7764.
2. Outten, C. E., and O'Halloran, T. V. (2001) Femtomolar sensitivity of metalloregulatory proteins controlling zinc homeostasis, *Science 292*, 2488−2492.
3. Rae, P. J., Schmidt, P. J., Pufahl, R. A., Culotta, V. C., and O'Halloran, T. V. (1999) Undetectable intracellular free copper: the requirement of a copper chaperone for superoxide dismutase, *Science 284*, 805−808.
4. Klomp, L. W. J., Lin, S.-J., Yuan, D. S., Klausner, R. D., Cizewski Culotta, V., and Gitlin, J. D. (1997) Identification and functional expression of HAH1, a novel human gene involved in copper homeostasis, *J. Biol. Chem. 272*, 9221−9226.
5. Hung, H. I., Casareno, R. L. B., Labesse, G., Mathews, F. S., and Gitlin, J. D. (1998) HAH1 is a copper binding protein with distinct amino acid residues mediating copper homeostasis and antioxidant defense, *J. Biol. Chem. 273*, 1749−1754.
6. Hamza, I., Schaefer, M., Klomp, L. W., and Gitlin, J. D. (1999) Interaction of the copper chaperone HAH1 with the Wilson disease protein is essential for copper homeostasis, *Proc. Natl. Acad. Sci. U.S.A. 96*, 13363−13368.
7. Wernimont, A. K., Huffman, D. L., Lamb, A. L., O'Halloran, T. V., and Rosenzweig, A. C. (2000) Structural basis for copper transfer by the metallochaperone for Menkes/Wilson disease proteins, *Nat. Struct. Biol. 7*, 766−771.
8. Walker, J. M., Tsivkovskii, R., and Lutsenko, S. (2002) Metallochaperone Atox1 transfers copper to the NH_2-terminal domain of the Wilson's disease protein and regulates its catalytic activity, *J. Biol. Chem. 277*, 27953−27959.
9. Ralle, M., Lutsenko, S., and Blackburn, N. J. (2003) X-ray absorption spectroscopy of the copper chaperone HAH1 reveals a linear 2-coordinate Cu(I) center capable of adduct formation with exogenous thiols and phosphines, *J. Biol. Chem. 278*, 23163−23170.
10. Glerum, D. M., Shtanko, A., and Tzagoloff, A. (1996) SCO1 and SCO2 act as high copy suppressors of a mitochondrial copper recruitment defect in *Saccharomyces cerevisiae*, *J. Biol. Chem. 271*, 20531−20535.
11. Nittis, T., George, G. N., and Winge, D. R. (2001) Yeast Sco1, a protein essential for cytochrome *c* oxidase function is a Cu(I)-binding protein, *J. Biol. Chem. 276*, 42520−42526.
12. Balatri, E., Banci, L., Bertini, I., Cantini, F., and Ciofi-Baffoni, S. (2003) Solution structure of Sco1: a thioredoxin-like protein involved in cytochrome *c* oxidase assembly, *Structure 11*, 1431−1443.
13. Tzagoloff, A., Capitanio, N., Nobrega, M. P., and Gatti, D. (1990) Cytochrome oxidase assembly in yeast requires the product of COX11, a homologue of the *P. denitrificans* protein encoded by ORF3, *EMBO J. 9*, 2759−2764.
14. Banci, L., Bertini, I., Cantini, F., Ciofi-Baffoni, S., Gonnelli, L., and Mangani, S. (2004) Solution structure of Cox11: a novel type of beta-mmunoglobulin-like fold involved in Cu_B site formation of cytochrome *c* oxidase, *J. Biol. Chem. 279*, 34833−34839.
15. Carr, H. S., George, G. N., and Winge, D. R. (2002) Yeast Cox11, a protein essential for cytochrome *c* oxidase assembly, is a Cu(I)-binding protein, *J. Biol. Chem. 277*, 31237−31242.
16. Glerum, D. M., Shtanko, A., and Tzagoloff, A. (1996) Characterization of *COX17*, a yeast gene involved in copper metabolism and assembly of cytochrome oxidase, *J. Biol. Chem. 271*, 14504−14509.
17. Beers, J., Glerum, D. M., and Tzagoloff, A. (1997) Purification, characterization and localization of yeast Cox17p, a mitochondrial copper shuttle, *J. Biol. Chem. 272*, 33191−33196.
18. Heaton, D. N., George, G. N., Garrison, G., and Winge, D. R. (2001) The mitochondrial copper metallochaperone Cox17 exists as an oligomeric polycopper complex, *Biochemistry 40*, 743−751.
19. Srinivasan, C., Posewitz, M. C., George, G. N., and Winge, D. R. (1998) Characterization of the copper chaperone Cox17 of *Saccharomyces cerevisiae*, *Biochemistry 37*, 7572−7577.
20. Culotta, V. C., Klomp, L. W. J., Strain, J., Casareno, R. L. B., Krems, B., and Gitlin, J. (1997) The copper chaperone for superoxide dismutase, *J. Biol. Chem. 272*, 23469−23472.
21. Casareno, R. L. B., Waggoner, D., and Gitlin, J. D. (1998) The copper chaperone CCS directly interacts with copper/zinc superoxide dismutase, *J. Biol. Chem. 273*, 23625−23628.
22. Hall, L. T., Sanchez, R. L., Holloway, S. P., Zhu, H., Stine, J. E., Lyons, T. J., Demeler, B., Schirf, V., Hansen, J. C., Nersissian, A. M., Valentine, J. S., and Hart, P. J. (2000) X-ray crystallographic and ultracentrifugation analyses of truncated and full-length copper chaperones for SOD (LYS7). A dimer−dimer model of LYS7−SOD association and copper delivery, *Biochemistry 39*, 3611−3623.
23. Rae, T. D., Torres, A. S., Pufahl, R. A., and O'Halloran, T. V. (2001) Mechanism of Cu, Zn-superoxide dismutase activation by the human metallochaperone hCCS, *J. Biol. Chem. 276*, 5166−5176.
24. Torres, A. S., Petri, V., Rae, T. D., and O'Halloran, T. V. (2001) Copper stabilizes a heterodimer of the yCCS metallochaperone and its target superoxide dismutase, *J. Biol. Chem. 276*, 38410−38416.
25. Tainer, J. A., Getzoff, E. D., Richardson, J. S., and Richardson, D. C. (1983) Structure and mechanism of copper, zinc superoxide dismutase, *Nature 306*, 284−287.
26. Hart, P. J., Balbirnie, M. M., Ogihara, N. L., Nersissian, A. M., Weiss, M. S., Valentine, J. S., and Eisenberg, D. (1999) A structure-based mechanism for copper−zinc superoxide dismutase, *Biochemistry 38*, 2167−2178.
27. McCord, J. M., and Fridovich, I. (1969) Superoxide dismutase. An enzyme function for erythrocuprein (hemocuprein), *J. Biol. Chem. 244*, 6049−6055.
28. Blackburn, N. J., Hasnain, S. S., Binsted, N., Diakun, G. P., Garner, C. D., and Knowles, P. F. (1984) An extended-X-ray-absorption-fine-structure study of bovine erythrocyte superoxide dismutase in aqueous solution. Direct evidence for three-coordinate Cu(I) in the reduced enzyme, *Biochem. J. 219*, 985−990.
29. Lepock, J. R., Arnold, L. D., Torrie, B. H., Andrews, B., and Kruuv, J. (1985) Structural analyses of various Cu^{2+}, Zn^{2+}-superoxide dismutases by differential scanning calorimetry and Raman spectroscopy, *Arch. Biochem. Biophys. 241*, 243−251.
30. Schmidt, P. J., Rae, T. D., Pufahl, R. A., Hamma, T., Strain, J., O'Halloran, T. V., and Culotta, V. C. (1999) Multiple protein domains contribute to the action of the copper chaperone for superoxide dismutase, *J. Biol. Chem. 274*, 23719−23725.
31. Lamb, A. L., Wernimont, A. K., Pufahl, R. A., Culotta, V. C., O'Halloran, T. V., and Rosenzweig, A. C. (1999) Crystal structure of the copper chaperone for superoxide dismutase, *Nat. Struct. Biol. 6*, 724−729.
32. Lamb, A. L., Torres, A. S., O'Halloran, T. V., and Rosenzweig, A. C. (2001) Heterodimeric structure of superoxide dismutase in complex with its metallochaperone, *Nat. Struct. Biol. 8*, 751−755.
33. Field, L. S., Furukawa, Y., O'Halloran, T. V., and Culotta, V. C. (2003) Factors controlling the uptake of yeast copper/zinc superoxide dismutase into mitochondria, *J. Biol. Chem. 278*, 28052−28059.
34. Brown, N. M., Torres, A. S., Doan, P. E., and O'Halloran, T. V. (2004) Oxygen and the copper chaperone CCS regulate posttranslational activation of Cu, Zn superoxide dismutase, *Proc. Natl. Acad. Sci. U.S.A. 101*, 5518−5523.

35. Furukawa, Y., Torres, A. S., and O'Halloran, T. V. (2004) Oxygen-induced maturation of SOD1: a key role for disulfide formation by the copper chaperone CCS, *EMBO J. 23*, 2872−2881.
36. Lamb, A. L., Wernimont, A. K., Pufahl, R. A., O'Halloran, T. V., and Rosenzweig, A. C. (2000) Crystal structure of the second domain of the human copper chaperone for superoxide dismutase, *Biochemistry 39*, 1589−1595.
37. Eisses, J. F., Stasser, J. P., Ralle, M., Kaplan, J., and Blackburn, N. J. (2000) Domains I and III of the human copper chaperone for superoxide dismutase interact via a cysteine-bridged dicopper cluster, *Biochemistry 39*, 7337−7342.
38. Zhu, H., Shipp, E., Sanchez, R., Liba, A., Stine, J. E., Hart, P. J., Gralla, E. B., Nersissian, A. M., and Valentine, J. S. (2000) Co(2+) binding to human and tomato copper chaperone for superoxide dismutase: Implications for the metal ion transfer mechanism, *Biochemistry 39*, 5413−5421.
39. Riggs, P. (1992) in *Short Protocols in Molecular Biology: A Compendium of Methods from Current Protocols in Molecular Biology* (Ausubel, F. A., Brent, R., Kingston, R. E., Moore, D. D., Seidman, J. G., Smith, J. A., and Struhl, K., Eds.) pp 16.6.1−16.6.14, Greene Publishing and Wiley, New York.
40. George, G. N. (1990) EXAFSPAK, Menlo Park, CA
41. Binsted, N., Gurman, S. J., and Campbell, J. W. (1998) EXCURVE 9.2, Warrington, England.
42. Gurman, S. J., Binsted, N., and Ross, I. (1984) A rapid, exact, curved-wave theory for EXAFS calculations, *J. Phys. C 17*, 143−151.
43. Gurman, S. J., Binsted, N., and Ross, I. (1986) A rapid, exact, curved-wave theory for EXAFS calculations. II. The multiple-scattering contributions, *J. Phys. C 19*, 1845−1861.
44. Binsted, N., and Hasnain, S. S. (1996) State of the art analysis of whole X-ray absorption spectra, *J. Synchrotron Rad. 3*, 185−196.
45. Blackburn, N. J., Rhames, F. C., Ralle, M., and Jaron, S. (2000) Major changes in copper coordination accompany reduction of peptidylglycine monooxygenase, *J. Biol. Inorg. Chem. 5*, 341−353.
46. Zabinsky, S. I., Rehr, J. J., Ankudinov, A. L., Albers, R. C., and Eller, M. J. (1995) Multiple-scattering calculations of X-ray-absorption spectra, *Phys. Rev. B. 52*, 2995−3009.
47. Blackburn, N. J., Hasnain, S. S., Diakun, G. P., Knowles, P. F., Binsted, N., and Garner, C. D. (1983) An extended X-ray-absorption-fine-structure study of the copper and zinc sites of freeze-dried bovine superoxide dismutase, *Biochem. J. 213*, 765−768.
48. Blackburn, N. J., Strange, R. W., McFadden, L. M., and Hasnain, S. S. (1987) Anion binding to bovine erythrocyte superoxide dismutase studied by XAS spectroscopy. A detailed structural analysis of native, azido- and cyano- derivatives using a multiple scattering approach, *J. Am. Chem. Soc. 109*, 7162−7170.
49. Kau, L. S., Spira-Solomon, D., Penner-Hahn, J. E., Hodgson, K. O., and Solomon, E. I. (1987) X-ray absorption edge determination of the oxidation state and coordination number of copper: Application to the type 3 site in *Rhus vernicifera* laccase and its reaction with oxygen, *J. Am. Chem. Soc. 109*, 6433−6422.
50. Blackburn, N. J., Strange, R. W., Reedijk, J., Volbeda, A., Farooq, A., Karlin, K. D., and Zubieta, J. (1989) X-ray absorption edge spectroscopy of copper(I) complexes. Coordination geometry of copper(I) in the reduced forms of copper proteins and their derivatives with carbon monoxide, *Inorg. Chem. 28*, 1349−1357.
51. Pickering, I. J., George, G. N., Dameron, C. T., Kurz, B., Winge, D. R., and Dance, I. G. (1993) X-ray absorption spectrsoscopy of cuprous-thiolate clusters in proteins and model systems, *J. Am. Chem. Soc. 115*, 9498−9505.
52. Ralle, M., Lutsenko, S., and Blackburn, N. J. (2004) Copper transfer to the N-terminal domain of the Wilson disease protein (ATP7B). X-ray absorption spectroscopy of reconstituted and chaperone-loaded metal binding domains and their interaction with exogenous ligands, *J. Inorg. Biochem. 98*, 765−779.

BI0478392